INVESTIGATING INCOMPLETE FUSION IN $^{12}C + ^{193}Ir$ SYSTEM*

Amanjot[a], Malika Kaushik[a], Priyanka Raizada[a]
Subham Kumar[a], Manoj Kumar Sharma[b], Rakesh Kumar[c]
Pushpendra P. Singh[a]

[a]Indian Institute of Technology Ropar, Rupnagar — 140 001, Punjab, India
[b]University of Lucknow, Lucknow — 226 007, UP, India
[c]Inter-University Accelerator Centre, New Delhi — 110 067, India

Received 9 November 2023, accepted 12 January 2024,
published online 24 April 2024

In this work, channel-by-channel excitation functions of evaporation residues, ^{201}Bi ($4n$), ^{201}Pb ($p3n$), and ^{198}Tl ($\alpha 3n$), populated via complete and/or incomplete fusion in the $^{12}C + ^{193}Ir$ system, have been measured at energies $\approx$ 64–84 MeV using an activation technique followed by the off-line γ-spectroscopy and compared with the PACE4 calculations. The reaction residues have been identified based on their characteristic γ-lines and decay curve analysis. The preliminary analysis suggests that the xn/pxn channels are predominantly populated via a complete fusion of ^{12}C with ^{193}Ir and α-emitting channels show a contribution from both the complete and incomplete fusion at the studied energy range.

DOI:10.5506/APhysPolBSupp.17.3-A26

1. Introduction

In heavy-ion (HI) induced reactions, in general, the complete fusion (CF) dominates around the Coulomb barrier energies. However, a substantial fraction of incomplete fusion (ICF) has been observed at these energies, owing to the interplay of different entrance-channel parameters [1, 2]. The input angular momentum associated with the impact parameters within the target dimensions leads to both the CF and ICF processes. In CF, when $\ell < \ell_{\rm crit}$, the attractive nuclear potential predominates over the sum of repulsive Coulomb and centrifugal potentials, resulting in the complete amalgamation of projectile and target nucleus, forming an excited compound nucleus (CN), which may decay via light nuclear particles and γ-rays. However, for $\ell > \ell_{\rm crit}$, as

* Presented at the XXXVII Mazurian Lakes Conference on Physics, Piaski, Poland, 3–9 September, 2023.

the energy of the incident projectile increases, the fusion pocket in the effective potential disappears, prompting the projectile to break up. One of the fragments fuses with the target nucleus, forming an incompletely fused composite system. The unfused fragment goes in the forward cone with projectile velocity without influencing the reaction process [3].

Despite various theoretical models given elsewhere [4] have been proposed to understand ICF dynamics, none have satisfactorily explained the ICF data below 8 MeV/nucleon. While these models have generally been applied to reproduce experimental data obtained at projectile energies $E/A \geq$ 10 MeV, the process of ICF has not been fully explained at relatively low bombarding energies, *i.e.*, 4–8 MeV/nucleon. The analysis of several experiments involving α-clustered ^{12}C projectile with various targets such as ^{128}Te [5], ^{181}Ta [6], ^{115}In [7], ^{159}Tb [8], ^{175}Lu [9], ^{165}Ho [10], and ^{197}Au [11] available in the literature suggests that the exact onset/threshold of ICF may/may not be defined based on consistent input entrance channel parameters such as projectile energy, mass asymmetry, Coulomb effect, projectile structure, and input angular momentum [12]. In most ICF studies, low-Z ($Z \leq 10$) projectiles have been used on light- to medium-mass targets. However, such information is scarce with heavy target ($A \geq 150$) nuclei. To investigate further, an experiment has been carried out at Inter-University Accelerator Centre (IUAC) in New Delhi, India to measure channel-by-channel excitation functions (EFs) of evaporation residues (ERs) populated in the ^{12}C+^{193}Ir reaction at $E_{\rm lab} \approx$ 64–84 MeV.

2. Experimental details

The isotopically pure ^{193}Ir (99.9% enriched) target foils of thickness 17–60 μg/cm^2, backed by 1–1.5 mg/cm^2 Al were fabricated [13]. Two stacks of four target-catcher assemblies were irradiated in a General Purpose Scattering Chamber (GPSC) using ^{12}C beams at 84 and 81 MeV, covering energies in the range of $E_{\rm lab} \approx$ 64–84 MeV. An electron-suppressed Faraday cup was employed to monitor the integrated beam current, allowing for correction due to variations in beam intensity throughout the irradiation, a crucial consideration for the short-lived radionuclides. A beam current of about 1 to 2 pnA was maintained throughout the irradiation. After the irradiation, the stacks were carefully removed from the GPSC using an in-vacuum transfer facility and counted off-line using two pre-calibrated high-purity germanium (HPGe) clover detectors coupled with a CAMAC-based DAQ system [14]. The γ-ray spectra have been analyzed using CANDLE [15]; refer to Fig. 1 for γ-spectra where peaks of interest are marked. To ensure accuracy, the HPGe clover detectors underwent energy and efficiency calibrations using a standard ^{152}Eu γ-ray source, illustrated in Fig. 2 (a). The ERs were identified by their characteristic γ-rays and further validated through decay-curve analysis. The decay curves of ^{201}Bi and ^{198}Tl are shown in Fig. 2 (b)–(d) as a representative case. The cross sections (σ) of the identified ERs were calculated using standard formulation given elsewhere [16]. The overall error associated with the cross section due to counting statistics, detection efficiency, variations in target thickness, and beam current fluctuations is estimated to be ≈ 10% to 15%.

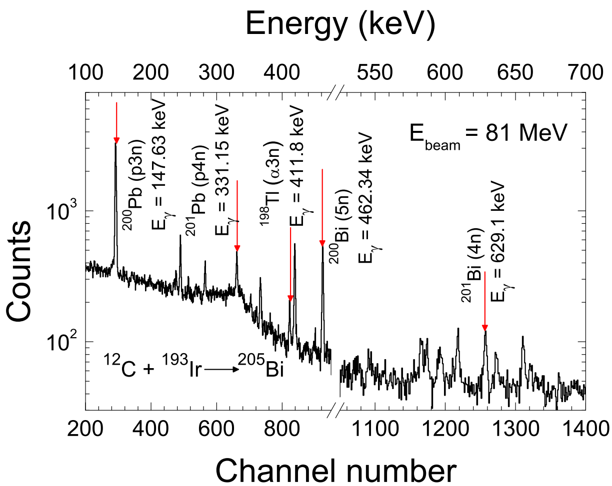

Fig. 1. γ-ray spectrum acquired at $E_{\mathrm{lab}} = 81$ MeV in ^{12}C+^{193}Ir system. γ-rays assigned to various ERs are marked.

3. Results and analysis

In the preliminary analysis of ^{12}C+^{193}Ir reaction data, the EFs of various ERs populated via CF and/or ICF are measured and analyzed using the statistical model code PACE4 [18]. This code accounts for the formation and decay of CN, primarily considering CF. Within the PACE4 code, the level density parameter is a crucial parameter, denoted as $a = A/K$ (where K is a free parameter), that plays a pivotal role in reproducing the cross sections of ERs.

Figure 3 (a) showcases the EF for the ^{201}Bi residue, expected to be formed through the emission of 4 neutrons from ^{205}Bi*. The experimental EF is compared with PACE4 for three different K values (*i.e.*, $K = 9, 11, 13$). As can be seen from this figure, EF of ^{201}Bi aligns exceptionally well with PACE4 when the value of K is set to 13. Consequently, $a = A/13$ MeV^{-1} has been assumed as the default value of the level density parameter within the studied energy range and can be used for analyzing other residues produced

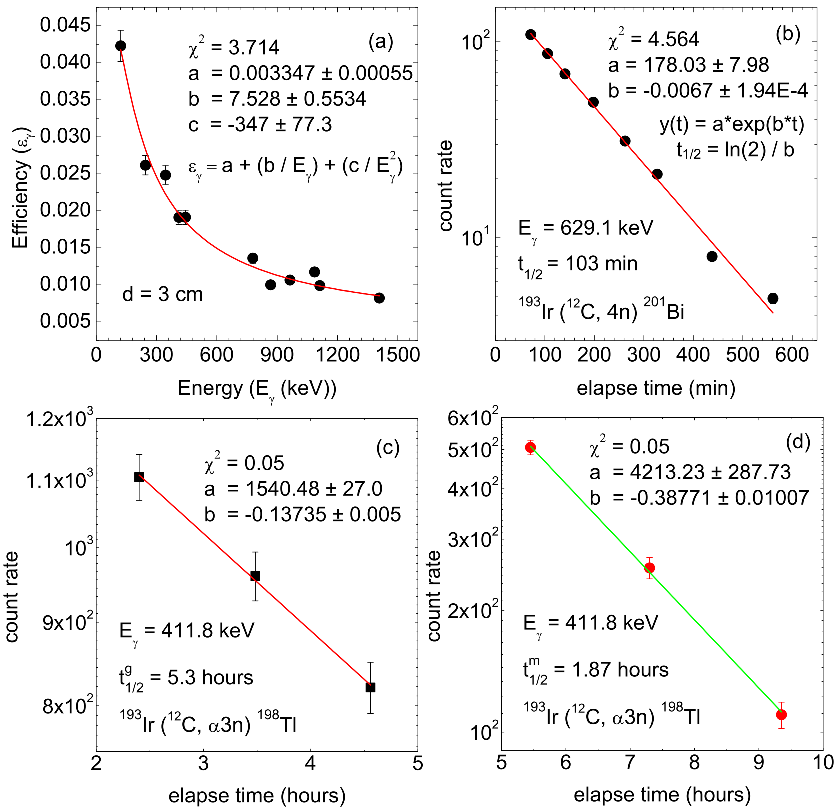

Fig. 2. (a) Experimental efficiency of the clover HPGe detector using ^{152}Eu γ-source at a source-to-detector distance $d = 3$ cm, (b) the decay curve for the ^{201}Bi obtained by following 629.1 keV γ-line, confirming a half-life of 103.4 minutes, (c) and (d) the decay curve for the ^{198}Tl having both the ground as well as metastable states, each with distinct half-lives of 5.04(4) hours and 1.78(4) hours, respectively, along with identical γ-ray (411.8 keV). The measured half-lives are consistent with the values listed in the literature [17]. The errors are included in the data plots; in panel (b), the errors are within the size of the data point.

in the ^{12}C+^{193}Ir system. Some residues are populated due to the decay of higher-charge isobar precursors via β^+ emission and/or electron capture. The formulation for extracting independent production cross sections from cumulative ones is given elsewhere [19]. The deduced independent cross section of ^{201}Pb is shown in Fig. 3 (b), and it matches well with the theoretical predictions. Further, the EFs of ^{201}Bi and ^{201}Pb have been compared with the PACE4 predictions using $K = 13$, exhibiting reasonable agreement, indicating the population of these residues through the CF process.

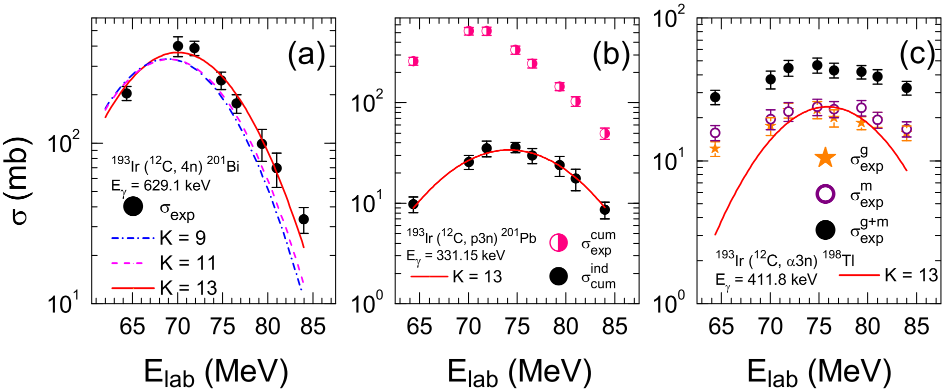

Fig. 3. Experimental EFs of (a) ^{201}Bi ($4n$), (b) ^{201}Pb ($p3n$), and (c) ^{198}Tl ($\alpha 3n$) residues juxtaposed with the predictions of PACE4 using a value of level-density parameter $a = A/13$ MeV^{-1}.

In this work, ^{198}Tl has both the metastable and ground states, each with distinct half-lives of 1.87 hours and 5.3 hours, along with identical γ-ray (411.8 keV) having different branching ratios (59.0% and 80.0 %) associated with each state. The cross sections for both states are measured separately, and the total cross section is determined by summing the contributions from both metastable and ground states and presented in Fig. 3 (c). The experimental cross sections are compared with PACE4. As shown in this figure, the cumulative $(m + g)$ experimental cross sections of ^{198}Tl residue are notably higher as compared to the PACE4 estimations across the entire energy range under investigation, indicating the population of this residue via both the CF and ICF processes. As PACE4 does not account for breakup/ICF reactions, it is plausible that the population of α-emitting channels involves contributions from the ICF processes. ICF has been attributed to the relatively low α separation energy ($\sim$ 7.3 MeV) associated with the ^{12}C projectile. In such a configuration, ^{12}C is inclined to break apart into two primary fragments: ^{8}Be and an α-particle. This breakup mechanism provides insights into the observed ICF phenomena in these systems [20].

4. Summary and conclusions

In summary, the EFs for various ERs populated via CF and/or ICF in the ^{12}C+^{193}Ir system have been measured at energies $E_{\rm lab} \approx$ 64–84 MeV using the recoil-catcher activation technique followed by the off-line γ-spectroscopy, and compared with the PACE4 predictions for different values of level density parameters. A value of level density parameter, $a = A/13$ MeV^{-1}, has been optimized as the default value within the studied energy range, which can be used as a base value to analyze $xn/pxn/\alpha xn$ channels produced via CF. The overall error in the measured cross sections is estimated to be $\leq 15\%$. It has been found that most of the non-α-emitting channels are populated via CF; however, α-emitting channels seem to have contributions from both CF and ICF. The α-cluster configuration of ^{12}C projectile significantly influences the onset of ICF channels in this reaction. Given the literature, it has been found that the ICF studies are confined to light- and medium-mass targets, and ICF contributes a small fraction to the total fusion. However, very few studies with heavy targets are available. It has been found that the ICF substantially contributes to the reaction cross-sections. The effect of various entrance channel parameters on the onset and strength of ICF will be investigated at low incident energies in the remaining analysis.

The authors acknowledge IUAC New Delhi for experimental facilities. One of the authors, Amanjot, thanks the Department of Science & Technology, Government of India, for the INSPIRE fellowship for her doctoral thesis.

REFERENCES

[1] P.P. Singh *et al.*, *Phys. Rev. C* **77**, 014607 (2008), and references therein.
[2] R.N. Sahoo *et al.*, *Nucl. Phys. A* **983**, 145 (2019).
[3] A.K. Nasirov *et al.*, *Phys. Lett. B* **842**, 137976 (2023).
[4] P.P. Singh *et al.*, *Eur. Phys. J. A* **34**, 29 (2007).
[5] M.K. Sharma *et al.*, *J. Phys. Soc. Jpn.* **72**, 1917 (2003).
[6] P. Kaur *et al.*, *Phys. Rev. C* **105**, 014629 (2022).
[7] S. Mukherjee *et al.*, *Int. J. Mod. Phys. E* **15**, 237 (2006).
[8] A. Yadav *et al.*, *Phys. Rev. C* **85**, 034614 (2012).
[9] H. Kumar *et al.*, *Nucl. Phys. A* **960**, 53 (2017).
[10] S.A. Tali *et al.*, *Phys. Rev. C* **100**, 024622 (2019).
[11] P. Kaur *et al.*, *Eur. Phys. J. Plus* **137**, 1287 (2022).
[12] A. Yadav *et al.*, *Phys. Rev. C* **96**, 044614 (2017).
[13] Amanjot *et al.*, to be published in *Vacuum*, 2023.
[14] E.T. Subramanium *et al.*, *Rev. Sci. Inst.* **77**, 096102 (2006).
[15] CANDLE, `http://www.iuac.res.in/NIAS/?url=Downloads/`
[16] M. Kaushik *et al.*, *Phys. Rev. C* **101**, 034611 (2020).
[17] `https://www.nndc.bnl.gov/nudat3/`
[18] LISE++, `https://lise.nscl.msu.edu/lise.html`
[19] I.M. Bhat *et al.*, *Phys. Rev. C* **105**, 054607 (2022).
[20] M. Sagwal *et al.*, *Phys. Rev. C* **107**, 034609 (2023).